

Active-site mutagenesis of a Lys⁴⁹-phospholipase A₂: biological and membrane-disrupting activities in the absence of catalysis

Richard J. WARD^{*1}, Lucimara CHIOATO[†], Arthur H. C. DE OLIVEIRA[‡], Roberto RULLER[†] and Juliana M. SÁ[†]

^{*}Departamento de Química, FFCLRP-USP, Universidade de São Paulo, Brazil, [†]Departamento de Bioquímica e Imunologia, FMRP-USP, Universidade de São Paulo, Brazil, and [‡]Departamento de Biologia Celular e Molecular e Bioagentes Patogênicos, FMRP-USP, Universidade de São Paulo, Brazil

Bothropstoxin-I (BthTx-I) is a myotoxic phospholipase A₂ variant present in the venom of *Bothrops jararacussu*, in which the Asp⁴⁹ residue is replaced with a lysine, which damages artificial membranes by a Ca²⁺-independent mechanism. Wild-type BthTx-I and the mutants Lys⁴⁹ → Asp, His⁴⁸ → Gln and Lys¹²² → Ala were expressed in *Escherichia coli* BL21(DE3) cells, and the hydrolytic, myotoxic and membrane-damaging activities of the recombinant proteins were compared with native BthTx-I purified from whole venom. The Ca²⁺-independent membrane-damaging and myotoxic activities of the native and wild-type recombinant BthTx-I, His⁴⁸Gln and Lys⁴⁹Asp mutants were similar; however, the Lys¹²²Ala mutant demonstrated reduced levels of both activities. Although a low hydrolytic activity against a mixed phospholipid substrate was observed with native

BthTx-I, no substrate hydrolysis was detected with the wild-type recombinant enzyme or any of the mutants. In the case of the Lys⁴⁹Asp mutant, this demonstrates that the absence of catalytic activity in Lys⁴⁹-PLA₂ is not a consequence of the single Asp⁴⁹ → Lys replacement. Furthermore, these results provide unambiguous evidence that the Ca²⁺-independent membrane-damaging and myotoxic activities are maintained in the absence of hydrolysis. The evidence favours a model for a hydrolysis-independent, membrane-damaging mechanism involving an interaction of the C-terminal region of BthTx-I with the target membrane.

Key words: bothropstoxin-I, calcium-independent activity, myotoxin.

INTRODUCTION

Phospholipases A₂ (PLA₂s; EC 3.1.1.4) catalyse the hydrolysis of the *sn*-2 acyl bonds of *sn*-3 phospholipids [1], and are currently classified into 11 Groups on the basis of amino acid sequence similarity [2]. The hydrolysis of phospholipids by Group I/II PLA₂s involves a His⁴⁸/Asp⁹⁹ pair in the catalytic site, which activate a structurally conserved water molecule, thereby initiating the nucleophilic attack on the *sn*-2 position of the substrate. During catalysis, the tetrahedral intermediate is stabilized by a Ca²⁺ ion cofactor, which is bound by the carboxyl oxygen atoms of Asp⁴⁹ and carbonyl main-chain oxygens of the neighbouring calcium-binding loop [3,4]. In the current consensus model of phospholipid hydrolysis, it is suggested that charge neutralization of the oxyanion intermediate alone is not sufficient to promote catalysis, and it has been proposed that an additional Ca²⁺ ion acts as an auxiliary electrophile, polarizing the amide of the Cys²⁹-Gly³⁰ peptide bond, which permits completion of the catalytic cycle [4].

A sub-family of class IIB PLA₂s have been purified from the venoms of several Asiatic and New World Viperid snakes, in which the Asp⁴⁹ residue is replaced by lysine [5,6]. Initial reports suggested that these Lys⁴⁹-PLA₂s retained low levels of catalytic activity [7–10]; however, subsequent studies failed to detect hydrolysis of phospholipid substrates [11–14]. Results from these later studies appeared to be supported by evidence from site-directed mutagenesis, which demonstrated that the replacement of Asp⁴⁹ with lysine in mammalian Asp⁴⁹-PLA₂s effectively eliminates catalytic activity [15–17]. Nevertheless, hydrolytic activity against phospholipid substrates with an arachidonyl group at the *sn*-2 position [18,19] or in the presence of

polycations [20] has been reported more recently, and uncertainty remains as to the levels and specificity of catalytic activity of the Lys⁴⁹-PLA₂s.

Crystal structures of Lys⁴⁹-PLA₂s have demonstrated that the ϵ -amino group of Lys⁴⁹ is located in the position occupied by the Ca²⁺ ion in Asp⁴⁹-PLA₂s [21–27], and it has been suggested that the reduction or elimination of catalytic activity results from either the re-orientation of the Cys²⁹-Gly³⁰ peptide bond [21], or reduced binding affinity of the Ca²⁺ cofactor [6,28]. However, the crystal structures of two Lys⁴⁹-PLA₂s have recently shown the presence of a fatty acid molecule bound in the substrate-binding cleft of the protein [25,27]. It was noted that the ϵ -amino group of Lys⁴⁹ could be sufficient to neutralize the formal negative charge of the oxyanion intermediate [27], and this has led to the suggestion that the ϵ -amino group of Lys¹²², which is favourably orientated in the majority of the Lys⁴⁹-PLA₂ structures, may serve as an auxiliary electrophile in substrate hydrolysis [27]. It was suggested further that, following cleavage of the *sn*-2 ester bond, Lys¹²² remains in position, thereby maintaining the Cys²⁹-Gly³⁰ peptide bond in a hyper-polarized state and trapping the fatty acid product in the active site [27]. In this model, although the Lys⁴⁹-PLA₂s might support phospholipid hydrolysis, they fail to release the fatty acyl product, resulting in an interrupted catalytic cycle [25,27]. Thus alternative interpretations of the structural evidence have been used to justify the absence, reduction or interruption of catalytic activity in the Lys⁴⁹-PLA₂s.

The Lys⁴⁹-PLA₂s demonstrate both Ca²⁺-independent membrane-damaging [29–31] and myotoxic activities [5,32]; however, the possible role of residual, interrupted or specific phospholipid hydrolysis in these activities is still an open question. With the aim of addressing these issues, we have

Abbreviations used: ASPC, 1-stearoyl-2-arachidonyl-*sn*-glycero-3-phosphocholine; BthTx-I, bothropstoxin-I; ITFE, intrinsic tryptophan fluorescence emission; rBthTx-I, recombinant bothropstoxin-I; CK, creatine kinase; DMPA, dimyristoylphosphatidic acid; EYPC, egg-yolk phosphatidylcholine; (Lys⁴⁹-/Asp⁴⁹-)PLA₂s, phospholipase A₂ with either lysine or aspartate at residue position 49; R_h, hydrodynamic radius.

¹ To whom correspondence should be addressed (e-mail rjward@fmrp.usp.br).

adopted as a model system the toxin bothropstoxin-I (BthTx-I), a Lys⁴⁹-PLA₂ that is present in the venom of the Viperid snake *Bothrops jararacussu* [32]. An expression system in *Escherichia coli* for BthTx-I has been developed recently [33], and here we describe the production and functional characterization of point mutants in the active-site and C-terminal regions, which have been used to evaluate and advance the current understanding of structure–function relationships in Lys⁴⁹-PLA₂s.

EXPERIMENTAL

Site-directed mutagenesis

A complete cDNA encoding BthTx-I has been isolated previously from venom gland cDNA by reverse transcriptase-PCR [34] (GenBank® accession No. X78599). In order to express the protein, restriction sites for *Nco*I and *Hind*III at the 5′ and 3′ extremities respectively, together with a stop codon at the 3′ end, were introduced by site-directed mutagenesis using the unique site-elimination protocol [35]. Sub-cloning of the *Nco*I–*Hind*III fragment into the equivalent restriction sites of the expression vector pET3-d introduced an N-terminal Met–Ala extension of the translated protein sequence; therefore this alanine codon was deleted by an additional round of site-directed mutagenesis. Nucleotide sequencing confirmed the desired final construct, in which Ser¹ of the BthTx-I is preceded by a methionine, and a stop codon immediately follows Cys¹³³ (the amino acid numbering throughout this report is in keeping with that reported previously for mammalian pancreatic PLA₂s; [36]).

After linearization of this construct with *Sca*I, site-directed mutagenesis of the BthTx-I was performed by PCR mutagenesis [37] to introduce the single mutations His⁴⁸ → Gln (oligonucleotide 5′-GTAACAGCATTTCTGCACGTAGCAGC-3′), Lys⁴⁹ → Asp (5′-GTAACAGCAATCGTGCACGTAGC-3′) and Lys¹²² → Ala (5′-GCAAAAAGGTGCCAGGTGATA-3′; the changed bases are shown underlined). The PCR reactions were performed using oligonucleotides complementary to the vector sequences flanking the BthTx-I insert, which contained restriction sites for *Xba*I (5′-extremity) and *Bam*HI (3′-extremity). After digestion with these enzymes, the final amplified fragments were sub-cloned into the equivalent sites in the expression vector pET3-d. All constructs were fully sequenced to confirm the introduction of the correct mutant and the absence of random mutagenesis resulting from a misreading of the DNA by *Taq* DNA polymerase.

Recombinant protein expression and purification

Of the growth medium [2.5 g of yeast extract/10 mM MgSO₄ (pH 7.5)/15 μg · l⁻¹ chloramphenicol/150 μg · l⁻¹ ampicillin], 150 ml was inoculated with *E. coli* strain BL21(DE3)pLysS transformed with the native or mutant constructs, and grown at 37 °C to a *D*₆₀₀ of 0.6. Recombinant protein expression was induced by addition of 0.6 mM isopropyl β-D-thiogalactoside ('IPTG'), and the culture was grown for an additional 5 h. Inclusion bodies were isolated from bacterial pellets by repeated rounds of sonication in 20 ml of lysis buffer [50 mM Tris/HCl (pH 8.0)/1 mM EDTA/1% (v/v) Triton X-100], followed by centrifugation at 12000 *g*. The protocol for the solubilization, refolding and purification by reversed-phase chromatography of recombinant BthTx-I was performed as described previously [33].

Spectroscopic characterization

All measurements were performed in 20 mM Hepes, pH 7.0/150 mM NaCl at 25 °C. Far-UV CD spectra (200–250 nm)

were measured with a JASCO 810 spectrometer (JASCO Inc., Tokyo, Japan) using 2 mm path-length cuvettes and protein concentrations of 150 μg · ml⁻¹ (native) and 70 μg · ml⁻¹ (recombinant) BthTx-I. A total of nine spectra were collected, averaged and corrected by subtraction of a buffer blank. Intrinsic tryptophan fluorescence emission (ITFE) spectra were measured between 300 and 450 nm with an excitation wavelength of 295 nm using a Spectronic 8100C spectrofluorimeter (Spectronic Instruments, Urbana, IL, U.S.A.) and a protein concentration of 30 μg · ml⁻¹. Excitation and emission slit widths were set at 4 nm with a photomultiplier tube voltage of 600 V, and all spectra were corrected by subtraction of a buffer blank. Protein hydrodynamic radius (*R*_h) was estimated by dynamic light scattering using a DynaPro MSTC014 (Protein Solutions, High Wycombe, Bucks., U.K.) at a protein concentration of 500 μg · ml⁻¹. All solutions were passed through a 0.22 μm filter, and centrifuged at 10000 *g* for 30 min before data collection. Data were acquired by accumulation of 82 scans of approx. 1.5 s, and the particle size distribution was calculated using the software package DYNAMCIS supplied with the instrument.

Release of entrapped fluorescent markers from liposomes

Membrane-damaging activity was evaluated by the release of the liposome-entrapped self-quenching fluorescent dye calcein. The loss of liposome membrane integrity results in dilution of the fluorophore with a consequent increase in the fluorescence signal [30,38]. Liposomes composed of a 9:1 molar ratio of egg-yolk phosphatidylcholine (EYPC):dimyristoylphosphatidic acid (DMPA) were prepared by reversed-phase evaporation in a buffer [150 mM NaCl/25 mM Hepes (pH 7.0)] containing 25 mM calcein (Sigma). The liposomes were passed through a 400 nm polycarbonate filter, and applied to a Sephadex G50 column (1 cm × 8 cm) to separate the liposomes from the free calcein. Proteins and liposomes were mixed to a final protein:lipid molar ratio of 1:200, and the kinetics of membrane damage were monitored by the increase in fluorescence emission at 520 nm with excitation at 490 nm. The fluorescence signal was expressed as the percentage of total calcein liberation on addition of 5 mM Triton X-100.

Myotoxic activity

Protein (30 μg) in a total volume of 50 μl of PBS was injected into the gastrocnemius muscle of male Swiss mice (body weight 18–22 g). After 3 h, a blood sample was collected from the tail in a heparinized capillary tube, and the plasma was separated by centrifugation. The plasma creatine kinase (CK) activity was determined using 4 μl of plasma with the CK-UV kinetic kit (Sigma Chemical Co.), following the manufacturer's instructions. Plasma CK activity was expressed in units · l⁻¹, where one unit is defined as the amount of enzyme that produces 1 mM of NADH · min⁻¹ under the standard conditions used in the assay. Animals used as negative controls received 50 μl of PBS, and all results were expressed as the mean plasma CK activity in a minimum of five experiments.

Evaluation of catalytic activity

Hydrolysis of phospholipids at the *sn*-2 position generates lysophospholipids and free fatty acids, which results in a decrease in the pH of the solution. The pH decrease was monitored by the decrease in absorption of Phenol Red (Merck) at 558 nm caused by protonation of the conjugate base [39]. EYPC (Calbiochem, San Diego, CA, U.S.A.) at a concentration of 300 μM solubilized in 4 mM cholate was used as substrate, with a final Phenol Red

concentration of 45 μM . Reaction kinetics in 150 mM NaCl at pH 7.5, in both the presence and absence of 10 mM CaCl₂, were monitored by measuring the absorption change at 558 nm after rapid mixing using an Applied Photophysics SX.18MV stopped-flow apparatus (Leatherhead, Surrey, U.K.) operated in the absorption mode. After the initial power-up, the instrument was left idle for a period of at least 30 min, and subsequently all experiments were performed at 25 °C in a nitrogen environment. Control experiments were performed using piratoxin III, a catalytically active Asp⁴⁹-PLA₂ purified from the venom of *Bothrops pirajai* under identical assay conditions. Catalytic activity was estimated directly from the kinetics of the change in absorption by calculation of concentration changes of the Phenol Red conjugate acid using the Henderson–Hasselbach equation, assuming a pK_a of 7.6 and a molar absorption coefficient (ϵ) at 558 nm of 60 580 M⁻¹ · cm⁻¹ for Phenol Red, and an optical path length of 0.2 cm.

RESULTS

The three-dimensional structure of the native BthTx-I has been determined previously [23], and Figure 1 shows a ribbon representation of the dimeric form of the protein. The inset to Figure 1 illustrates details of the active site and C-terminal regions, showing the side chain orientations of the Lys⁴⁹ and Lys¹²² residues, which are situated on opposite sides of the Ca²⁺-binding loop. The ϵ -amino group of the Lys⁴⁹ side chain forms hydrogen bonds with the main-chain carbonyl oxygen atoms of residues Asn²⁸ and Gly³⁰, whereas the ϵ -amino group of Lys¹²² forms a hydrogen bond with the main-chain carbonyl oxygen of Cys²⁹. The combination of the hydrogen-bonding patterns of these two lysine residues is conserved in the majority of the Lys⁴⁹-PLA₂ crystal structures solved to date [13,23–27], and results in the main-chain amide NH of Gly³⁰ being orientated towards the solvent-exposed cleft formed by the active-site region. The position and orientation of the His⁴⁸ residue, together

with the Asp⁹⁹, Tyr⁵² (also shown in Figure 1) and other residues in the catalytic network, are highly conserved among the class I/II Asp⁴⁹ and Lys⁴⁹-PLA₂s [21]. The conservation of these key elements of the catalytic apparatus has been used as structural evidence to support a role for phospholipid hydrolysis in the biological functions of Lys⁴⁹-PLA₂s [27], and one of the principal aims of this study was to evaluate this suggestion using site-directed mutagenesis of selected residues in this region.

The expression and refolding method [33] has been applied to obtain both wild-type and mutant recombinant BthTx-I, with excellent reproducibility. Site-directed mutagenesis in the active-site region might result in structural perturbations of the molecule: therefore all recombinant proteins were evaluated and compared with the native BthTx-I purified from *B. jararacussu* venom using a series of spectroscopic techniques. As presented in Figure 2(A), the CD spectra of the native and all recombinant proteins are essentially identical, confirming that the secondary structure is conserved during the refolding and purification processes. A single tryptophan residue at position 77 contributes to the intermolecular contacts that stabilize the BthTx-I dimer, and the fluorescence signal from this residue is highly sensitive to tertiary structural changes at the interface region [23,38,40]. The ITFE spectra of the native, recombinant wild-type and mutant BthTx-I proteins are shown superimposed in Figure 2(B), which demonstrates that the micro-environments of the tryptophan residues, and therefore the tertiary structure of the dimer interface region, are conserved in all protein samples. BthTx-I forms stable homodimers at pH 7.0 [33,38], and the dynamic light-scattering experiments demonstrate R_h values of between 1.62 and 1.66 nm for the recombinant wild-type and mutant proteins, which are similar to the value of 1.66 nm identified for native BthTx-I. This R_h value corresponds to a molecular-mass range of 26.7–27.4 kDa, which is in close agreement with the calculated value of 27.4 kDa for the molecular mass of the BthTx-I dimer, assuming a molecular mass of 13.7 kDa for the monomeric form [14,34]. The results of these spectroscopic experiments dem-

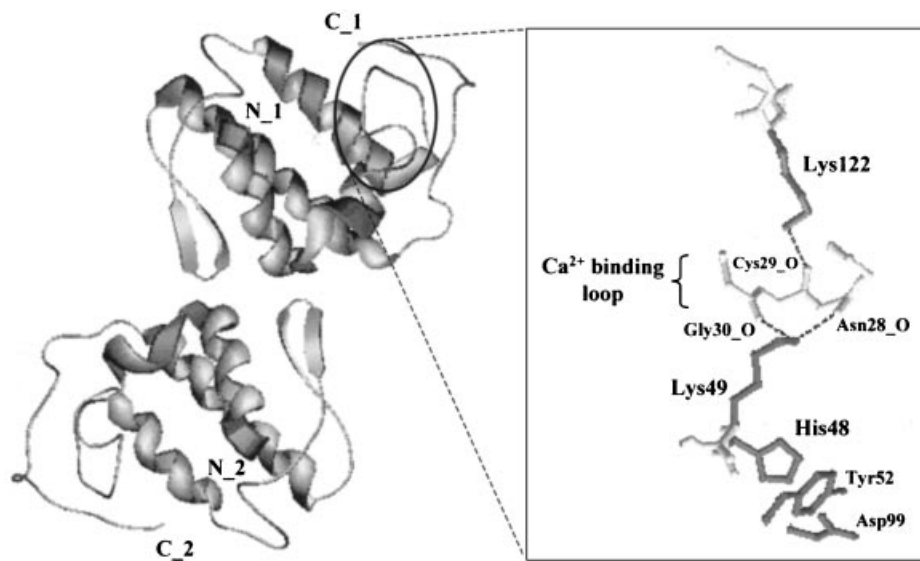


Figure 1 Three-dimensional structure of the BthTx-I dimer (left panel) and active-site region (right panel)

Left panel: ribbon representation of the BthTx-I dimer. The N- and C-termini of each monomer are indicated. Right panel: detail of the active-site and Ca²⁺-binding region of BthTx-I, in which main-chain atoms and bonds are shown in light grey, side chains are shown in dark grey, and hydrogen bonds are represented as dashed lines. The Figure was prepared using the graphics program Swiss-PDB viewer [57].

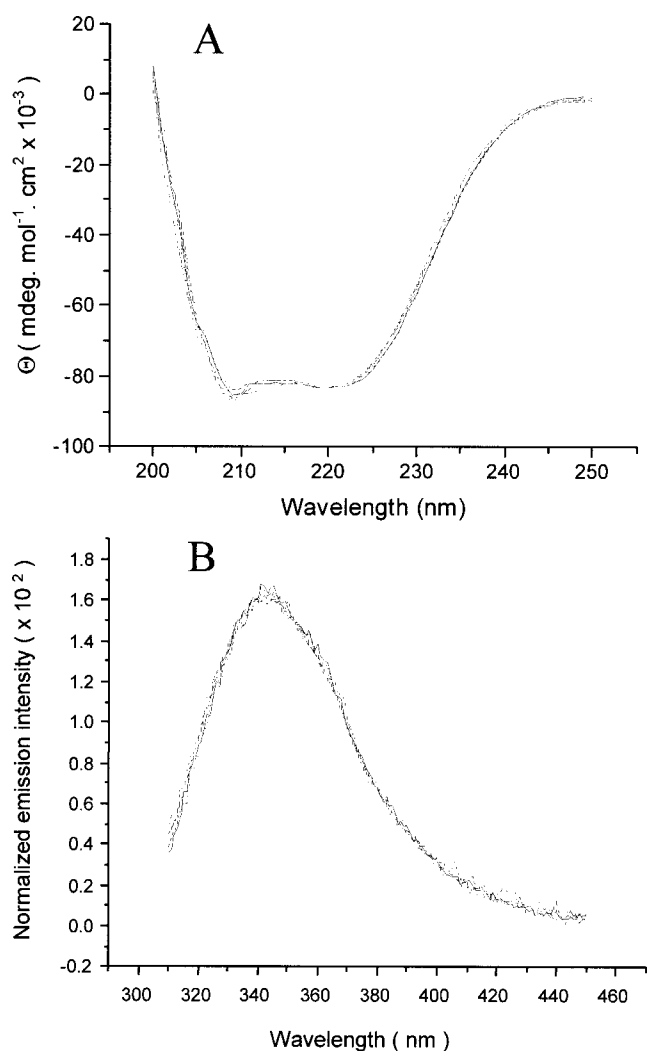


Figure 2 Far-UV CD spectra (A) and intrinsic tryptophan fluorescence emission spectra (B) of native BthTx-I, wild-type recombinant BthTx-I and mutants Lys⁴⁹Asp, His⁴⁸Gln and Lys¹²²Ala

The spectra measured in the near-UV CD (A) and intrinsic tryptophan fluorescence (B) experiments are shown superimposed, and are essentially identical. The protein concentrations used in the CD and fluorescence experiments were 150 $\mu\text{g} \cdot \text{ml}^{-1}$ and 30 $\mu\text{g} \cdot \text{ml}^{-1}$ respectively (see the Experimental section for further details).

onstrate that the secondary, tertiary and quaternary structures of the native, recombinant wild-type and mutant rBthTx-I proteins are indistinguishable. This conclusion is in agreement with previous site-directed mutagenesis results in bovine pancreatic class II Asp⁴⁹-PLA₂, which also demonstrated that mutations in the active-site region do not perturb significantly the global structure of the protein [16,41].

In addition to the spectroscopic characterization, the biological activities of the recombinant and native proteins were compared, and Figure 3 presents the myotoxic activity as monitored by the increase in plasma levels of CK. No significant differences in the myotoxic activities of the native BthTx-I, recombinant BthTx-I or the His⁴⁸Gln and Lys⁴⁹Asp mutants were observed, and these data provide further evidence that the native protein conformation is conserved in the recombinant protein. In the case of the Lys¹²²Ala mutant, the myotoxic activity is reduced by approx. 40%; however, it should be emphasized that the spectroscopic

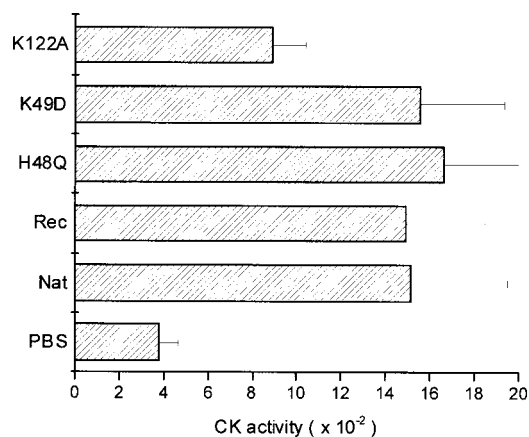


Figure 3 Myotoxic activity of native, wild-type recombinant and mutant BthTx-I as measured by intramuscular CK release

Plasma levels of CK activity were measured after injection of 30 μg of native (Nat), wild-type recombinant (Rec) or mutant BthTx-I (as indicated in the Figure). The plasma level of CK activity after injection of PBS is also shown. The results are presented as the means \pm S.D. for at least five measurements.

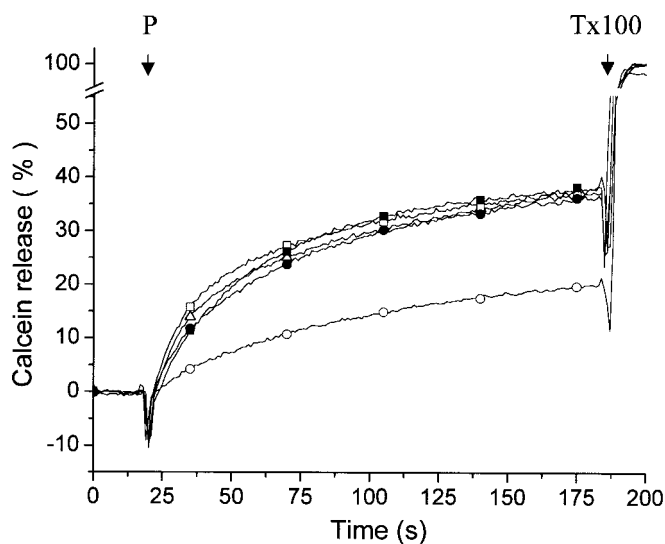


Figure 4 Ca²⁺-independent membrane-damaging activity of native, wild-type recombinant and mutant BthTx-I as measured by entrapped fluorescent marker release

Release kinetics of the fluorescent marker calcein from liposomes composed of a 9:1 molar ratio of EYPC and DMPA induced by native (\square), wild-type recombinant (\blacksquare), Lys⁴⁹Asp (\triangle), His⁴⁸Gln (\bullet) and Lys¹²²Ala (\circ) BthTx-I. The increase in the fluorescence signal on addition of protein (indicated by 'P' in the Figure) was monitored at $\lambda_{em} = 520$ nm with $\lambda_{ex} = 480$ nm, and is presented as the percentage of total dye liberation after addition of 5 mM Triton X-100 (Tx100).

characteristics of this mutant are unchanged in comparison with the other recombinant proteins used in this study. This result suggests that the effect on myotoxic activity observed in the Lys¹²²Ala mutant is functionally significant, and provides direct evidence that a structural motif in the C-terminal region of BthTx-I is a determinant of biological activity.

In addition to myotoxic activity, BthTx-I also damages artificial membranes via a Ca²⁺-independent mechanism, which, in

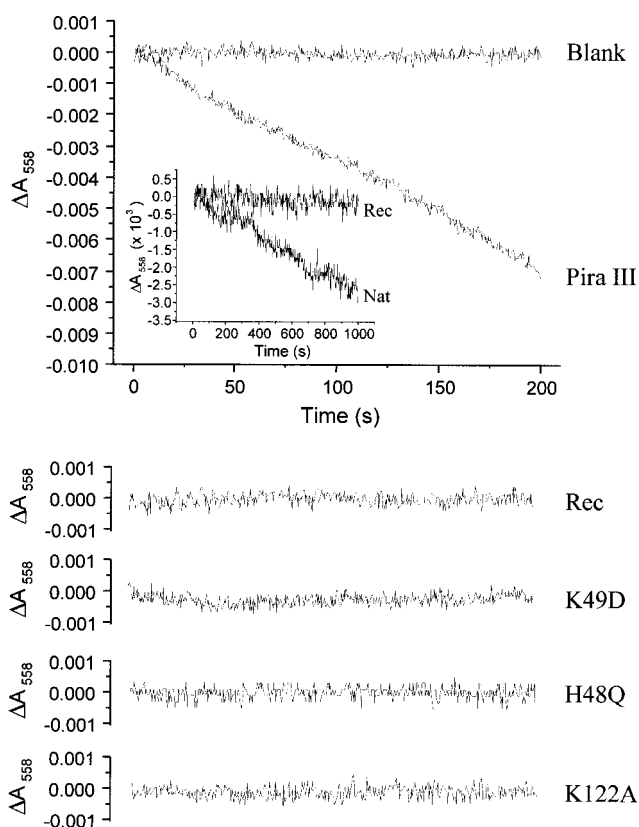


Figure 5 Phospholipid hydrolysis kinetics of native, wild-type recombinant and mutant BthTx-I as measured by stopped-flow spectroscopy

Upper panel: kinetics of the hydrolytic activity of piratoxin-III (Pira III), an Asp⁴⁹-PLA₂ from *B. pirajai*, against the EYPC substrate at a protein concentration of 1.5 μg · ml⁻¹, as measured with stopped-flow spectroscopy by the absorption change of Phenol Red at 558 nm. The control experiment in the absence of protein is also shown (Blank). Inset: long-time-base experiments showing hydrolysis kinetics of the native (Nat) and wild-type recombinant (Rec) BthTx-I at a protein concentration of 100 μg · ml⁻¹. Lower panel: hydrolysis kinetics of the EYPC substrate measured with the wild-type recombinant BthTx-I (Rec) and the mutants Lys⁴⁹Asp, His⁴⁸Gln and Lys¹²²Ala (indicated on the Figure) at a final protein concentration of 15 μg · ml⁻¹.

contrast with other class II Asp⁴⁹-PLA₂s, does not involve detectable phospholipid hydrolysis [30,31]. Kinetic measurements of entrapped fluorescent marker release from liposomes for native and recombinant wild-type BthTx-I, together with the His⁴⁸Gln, Lys⁴⁹Asp and Lys¹²²Ala mutants, are presented in Figure 4. The release kinetics of the native and recombinant wild-type proteins and the Lys⁴⁹Asp and His⁴⁸Gln mutants all revealed a rapid membrane-damaging activity, resulting in the release of 35–37% of the entrapped fluorescent marker, and these kinetic properties are similar to those reported previously for Lys⁴⁹-PLA₂s [29,30,38]. In contrast, the rate of marker release by the Lys¹²²Ala mutant was significantly reduced in comparison with the native protein, resulting in ≈ 19% marker release over the time course of the experiment. These data suggest that the C-terminal loop region of the protein is important not only as a determinant of biological activity, but also plays a role in the Ca²⁺-independent membrane-damaging mechanism.

Results of the hydrolytic activity assay using a mixed phospholipid substrate are presented in Figure 5, in which the upper panel shows the hydrolysis kinetics of EYPC by piratoxin-III, an Asp⁴⁹-PLA₂ from the venom of *B. pirajai*. The rate of free fatty acid release calculated using the Henderson–Hasselbach equation

yielded a specific activity of 42.3 μmol · min⁻¹ · mg⁻¹, and is similar to the value of 38.7 μmol · min⁻¹ · mg⁻¹ reported previously using the ‘pH-stat’ technique with the same substrate [42]. In the absence of Ca²⁺ (results not shown), the kinetics are indistinguishable from those the blank control experiment, in which substrate and buffer alone are mixed. The activity of native BthTx-I purified from the venom of *B. jararacussu* was measured in experiments over a long time course, in which a low level of hydrolytic activity was detected (approx. 0.2 μmol · min⁻¹ · mg⁻¹; inset to Figure 5, upper panel), which was abolished in the absence of Ca²⁺. This result is in contrast with previous observations using the pH-stat method, in which no hydrolytic activity with the native BthTx-I was detected using the same substrate [32,42], and highlights the often-contradictory nature of reports concerning the hydrolytic activities of Lys⁴⁹-PLA₂s purified from crude venoms. The observed dependence of the hydrolytic activity on Ca²⁺ led us to speculate that, even after re-purification, the hydrolytic activity of trace contaminants of Asp⁴⁹-PLA₂s present in the snake venom could be detected. This conclusion is supported by the hydrolysis kinetics results measured over a long period of time with the recombinant BthTx-I at a concentration of 100 μg · ml⁻¹ in the presence of Ca²⁺, in which no detectable hydrolytic activity was detected (Figure 5, upper panel, inset). These are the first reported results of a hydrolytic activity assay for a recombinant form of Lys⁴⁹-PLA₂ which, on the basis of the sensitivity of the technique, limits the hydrolytic activity of BthTx-I to < 0.002 μmol · min⁻¹ · mg⁻¹ under the experimental conditions described. The results of hydrolytic activity assays with the His⁴⁸Gln, Lys⁴⁹Asp and Lys¹²²Ala mutants are also presented in the lower panel of Figure 5. No phospholipid hydrolysis was detected in the presence of Ca²⁺ with any of the mutants; indeed, experiments performed over a long time period (1000 s) with all recombinant proteins produced kinetic traces that were indistinguishable from that of the control experiment in the absence of protein.

DISCUSSION

The availability of a simple and reproducible refolding protocol for BthTx-I [33] has, for the first time, enabled a critical evaluation of the current understanding of the structural basis of several aspects of Lys⁴⁹-PLA₂ function using site-directed mutagenesis. Previous studies using Lys⁴⁹-PLA₂s purified from crude venom extracts have provided inconclusive evidence with respect to the levels of hydrolytic activity [7–14,18–20] and, consequently, the question concerning the potential biological role of catalytic activity of the Lys⁴⁹-PLA₂s is a recurrent issue [44,45]. We have developed a sensitive detection assay for PLA₂ on the basis of the decrease in absorption of Phenol Red on liberation of free fatty acids. The sensitivity limit of the technique is determined by the optical drift over the time course of the experiment, and the time lapse between the instrument power-up and data collection, together with continuous purging with N₂ to eliminate slow absorption changes due to atmospheric CO₂, have proven to be key factors in maintaining constant baselines. In long-time-base experiments, the optical drift could be limited to < 0.001 absorption unit over a 1000 s time course, which yields a calculated lower detection limit for fatty acid production of > 200 fmol · min⁻¹. The sensitivity of the stopped-flow assay described here therefore compares favourably with hydrolysis detection by fluorescence [43] and pH-stat [16] techniques.

In Asp⁴⁹ PLA₂s the His⁴⁸/Asp⁹⁹ residue pair together with the Ca²⁺ ion cofactor bound to Asp⁴⁹ serve to stabilize the oxyanion

reaction intermediate in the catalytic cycle [3,4]. This mechanism has been tested extensively by site-directed mutagenesis studies, and it has been demonstrated that replacement of His⁴⁸ with either asparagine or glutamine in mammalian Asp⁴⁹-PLA₂s results in basal levels of hydrolytic activity [15–17], and that replacement of Asp⁴⁹ with lysine produces similar effects [17,46,47]. Comparison of several Lys⁴⁹-PLA₂ crystal structures with those of Asp⁴⁹-PLA₂s shows a strict conservation of the side chain orientations of the His⁴⁸/Asp⁹⁹ pair, the Tyr⁵² and Tyr⁷³ residues in the catalytic network, together with a water molecule, which is positioned correctly to act as the nucleophile in catalysis [13,21,22]. The Lys⁴⁹-PLA₂ crystal structures reveal further that the ϵ -amino group of Lys⁴⁹ fills the volume occupied by the Ca²⁺ cofactor in the Asp⁴⁹-PLA₂s. We therefore reasoned that reversion of Lys⁴⁹ to aspartate in BthTx-I would result in the completion of a His⁴⁸/Asp⁹⁹/Asp⁴⁹ motif, with the consequent appearance of Ca²⁺-dependent hydrolytic activity. However, the absence of hydrolytic activity observed in the BthTx-I Lys⁴⁹Asp mutant demonstrates that the completion of the catalytic motif fails to revert the hydrolytic function to that observed in the Asp⁴⁹ PLA₂s. This result demonstrates that the loss of hydrolytic activity in the BthTx-I is not the result of the single replacement of Asp⁴⁹ with lysine, and implies that other structural factors play a key role in the loss of catalytic function. Indeed, amino acid sequence comparisons have revealed that Tyr²⁸ and Gly³¹ in the active site and Ca²⁺-binding loop regions of Asp⁴⁹-PLA₂s are replaced with Asn²⁸ and Leu³¹ in the Lys⁴⁹-PLA₂s [12,55,56].

It has been suggested that an interrupted catalytic cycle may increase the affinity of the Lys⁴⁹-PLA₂s for both biological and artificial membranes, and that acylation of the protein might act as an activation mechanism for both the myotoxic [30] and the Ca²⁺-independent membrane-damaging activities [48]. The consensus model for the Asp⁴⁹-PLA₂ catalytic mechanism suggests that the Ca²⁺-induced stabilization of the oxyanion intermediate is enhanced by a supplementary electrophile, which polarizes and maintains the Cys²⁹–Gly³⁰ peptide bond in the Ca²⁺-binding loop in an orientation which is favourable for catalysis [4]. Recent crystallographic studies have observed catalytically favourable orientations of the Cys²⁹–Gly³⁰ peptide bond in the majority of Lys⁴⁹-PLA₂ crystal structures [13,22–27], which raises questions as to the role of an auxiliary electrophile in the polarization of this bond in the Lys⁴⁹-PLA₂s. It has recently been suggested that Lys¹²² situated in the C-terminal loop region in the Lys⁴⁹-PLA₂s may act as such an electrophile, favourably orientating the Cys²⁹–Gly³⁰ peptide bond and thereby permitting phospholipid hydrolysis [27]. Furthermore, it was proposed that the hyperpolarized peptide bond leads to an increased affinity for the head group of the fatty acyl product, which becomes trapped in the active site, resulting in an interrupted catalytic cycle [27]. We reasoned that if this is the case, then substitution of Lys¹²² would result in the loss of the interrupted catalytic cycle and a consequent decrease in the biological and membrane-damaging activities. Indeed, the Lys¹²²Ala mutant demonstrated both decreased myotoxic and Ca²⁺-independent membrane-damaging activities, which might be interpreted as supportive evidence for activation of BthTx-I via an interrupted catalytic cycle. Although no hydrolytic activity was observed in the Lys¹²²Ala mutant, caution must be exercised in eliminating a role for an interrupted cycle on the basis of this result, since a consequence of the failure of fatty acid release would be the absence of hydrolytic activity, as measured by any technique based on the detection of pH change.

This question was addressed by further mutagenesis of the BthTx-I active-site region. In Asp⁴⁹-PLA₂s, the His⁴⁸Gln substitution effectively abolishes hydrolytic activity [17,46,47], and

provides key evidence in favour of charge transfer during hydrolysis. The results presented here show that, although the His⁴⁸Gln mutant of BthTx-I shows no catalytic activity, both the myotoxic and the Ca²⁺-independent membrane-damaging activities are unaffected. This demonstrates that the substitution of His⁴⁸, and the consequent elimination of any possible catalytic activity, does not influence the activity of BthTx-I on either biological or artificial membranes. These results therefore provide strong evidence that the myotoxic and Ca²⁺-independent membrane-damaging activities of the BthTx-I do not involve hydrolytic activity, as part of either a complete or an interrupted catalytic cycle.

This conclusion helps to clarify the interpretation of the results from previous functional studies with Lys⁴⁹-PLA₂s. Chemical modification of the His⁴⁸ residue with 4-bromophenylacetyl bromide in several Lys⁴⁹-PLA₂s reduces both the myotoxic and Ca²⁺-independent membrane-damaging activities [49,50]. Our results demonstrate that these effects are not due to the elimination of catalytic activity, but to as-yet-unidentified structural changes induced by the chemical modification [51]. In contrast, experiments demonstrating fatty acid release in cell cultures treated with Lys⁴⁹-PLA₂s have been interpreted either as the effect of hydrolysis of specific substrates found in biological membranes or activation of endogenous PLA₂ [45,52]. A specific hydrolytic activity towards 1-stearoyl-2-arachidonoyl-*sn*-glycero-3-phosphocholine (ASPC) by several Lys⁴⁹-PLA₂s has been reported previously [18,19], and therefore the catalytic activities of both the native and recombinant wild-type BthTx-I were measured using this substrate. Under the same conditions as described for EYPC, the native BthTx-I demonstrated very low levels of Ca²⁺-dependent activity against ASPC, whereas no activity was detected with the recombinant wild-type BthTx-I (results not shown). These results demonstrate that the low level of phospholipid hydrolysis observed with the native protein is not due to an inherent Ca²⁺-dependent catalytic activity of BthTx-I. Crude extracts of *B. jararacussu* venom contain a complex mixture of at least four Asp⁴⁹- and Lys⁴⁹-PLA₂s [32], and we therefore suggest that the low level of catalytic activity observed in the native BthTx-I purified from this mixture is due to trace impurities of one or more catalytically active Asp⁴⁹-PLA₂s. Although our data do not exclude the possibility of hydrolytic activity of the native BthTx-I against a specific substrate *in vivo*, the present study suggests that the fatty acid release observed in cell culture is due either to Asp⁴⁹-PLA₂ contamination of the samples used or to endogenous PLA₂ activation. Nonetheless, our results demonstrate unambiguously that hydrolysis does not have a role in either the myotoxic or the Ca²⁺-independent membrane-damaging activities.

The effects on the myotoxic and Ca²⁺-independent membrane-damaging activities of site-directed mutagenesis in the C-terminal region of BthTx-I provide further insights into the biological activities of the Lys⁴⁹-PLA₂s. We have suggested previously that conformation changes in the BthTx-I dimer may alter the position of the C-terminal loop of the membrane-bound form of the protein, resulting in disruption of the lipid bilayer [23]. The reduced Ca²⁺-independent membrane-damaging activity of the Lys¹²²Ala mutant supports this model, and demonstrates the importance of the C-terminal region in this mechanism. Although the C-terminal loop regions of many snake venom PLA₂s are rich in cationic residues, the Ca²⁺-independent membrane-damaging appears to be unique to the Lys⁴⁹-PLA₂s, which suggests that the interaction of this region with the membrane is a specific event which is determined by defined structural motifs in the protein. The concept of defined structural motifs in the C-terminal region is supported by the observation

of a reduced activity of the Lys¹²²Ala mutant *in vivo*, which suggests that this residue participates in a motif that acts as a structural determinant of myotoxic activity in the Lys⁴⁹-PLA₂s. This suggestion is in agreement with reports demonstrating the neutralization of myotoxicity of myotoxin-II, a Lys⁴⁹-PLA₂ from *B. asper*, by monoclonal antibodies against the C-terminal region [53], and the observation that C-terminal peptides from the same protein display myotoxic activity [54]. It is noteworthy that both the myotoxic and Ca²⁺-independent membrane activities are lowered in the Lys¹²²Ala mutant, and further mutagenesis studies of the C-terminal region are currently in progress to evaluate whether these two activities are correlated.

In conclusion, we have presented evidence demonstrating the absence of catalytic activity of the BthTx-I either *in vitro* or *in vivo*, and that the myotoxic and Ca²⁺-independent membrane-damaging activities are therefore independent of direct phospholipid hydrolysis by this protein. Furthermore, no evidence was found to support a role for activation of the BthTx-I via an interrupted catalytic cycle. Our results suggest that additional structural factors resulting from the presence of other unique substitutions in the active-site region in Lys⁴⁹-PLA₂s [12,55,56] contribute to the loss of catalytic function; however, the structural basis of the lack of catalytic function in the Lys⁴⁹-PLA₂s remains obscure. Nonetheless, the mutagenesis results support a model [23] in which the C-terminal region is implicated in the Ca²⁺-independent membrane damaging mechanism, and indicates further a structural role for this region in the determination of myotoxic activity.

We are grateful to Dr S. H. Andrião-Escarso and Dr J. R. Giglio for providing the samples of piratoxin-III, and to Dr Roy E. Larson for access to the stopped-flow apparatus. This work was supported by FAPESP (Fundação de Amparo a Pesquisa do Estado de São Paulo) [grants 96/11165-3 (to R. J. W.), 98/14568-7 (to L. C.), 97/14370-0 (to A. H. C. de O.), 98/14686-0 (to R. R.), 98/14569-3 (to J. M. S.)] and CNPq [grant 300725/98-1 (to R. J. W.)].

REFERENCES

- van Deenen, L. L. M. and de Haas, G. H. (1963) The substrate specificity of phospholipase A₂. *Biochim. Biophys. Acta* **70**, 538–553
- Six, D. A. and Dennis, E. A. (2000) The expanding superfamily of phospholipase A₂ enzymes: classification and characterization. *Biochim. Biophys. Acta* **1488**, 1–19
- Verheij, H. M., Volwerk, J. J., Jansen, E. H., Dijkstra, B. W. and de Haas, G. H. (1980) Methylation of histidine-48 in pancreatic phospholipase A₂. Role of histidine and calcium ion in the catalytic mechanism. *Biochemistry* **19**, 743–750
- Scott, D. L., White, S. P., Otwinowski, Z., Yuan, W., Gelb, M. H. and Sigler, P. B. (1990) Interfacial catalysis: the mechanism of phospholipase A₂. *Science* **250**, 1541–1546
- Gutiérrez, J. M. and Lomonte, B. (1995) Phospholipase A₂ myotoxins from *Bothrops* snake venoms. *Toxicon* **33**, 1405–1424
- Arni, R. K. and Ward, R. J. (1996) Phospholipase A₂ – a structural review. *Toxicon* **34**, 827–841
- Maraganore, J. M., Merutka, G., Cho, W., Welches, W., Kezdy, F. J. and Heinrickson, R. L. (1984) A new class of phospholipase A₂ with lysine in place of aspartate 49. *J. Biol. Chem.* **259**, 13839–13843
- Maraganore, J. M. and Heinrickson, R. L. (1986) The lysine-49 phospholipase A₂ from the venom of *Agkistrodon piscivorus piscivorus*. Relation of structure and function to other phospholipases A₂. *J. Biol. Chem.* **261**, 4797–4804
- Maraganore, J. M., Joseph, M. and Bailey, M. C. (1987) Purification and characterization of trichosanthin. Homology to the ricin A chain and implications as to mechanism of abortifacient activity. *J. Biol. Chem.* **262**, 11628–11633
- Dhillon, D. S., Condeira, E., Maraganore, J. M., Heinrickson, R. L., Benjamin, S. and Rosenberg, P. (1987) Comparison of enzymatic and pharmacological activities of lysine-49 and aspartate-49 phospholipases A₂ from *Agkistrodon piscivorus piscivorus* snake venom. *Biochem. Pharmacol.* **36**, 1723–1730
- Condeira, E., Fletcher, J. E., Rapuano, B. E., Yang, C. C. and Rosenberg, P. (1981) Dissociation of enzymatic activity from lethality and pharmacological properties by carbamylation of lysines in *Naja nigricollis* and *Naja naja atra* snake venom phospholipases A₂. *Toxicon* **19**, 705–720
- Francis, B., Gutiérrez, J. M., Lomonte, B. and Kaiser, I. I. (1991) Myotoxin II from *Bothrops asper* (Terciopelo) venom is a lysine-49 phospholipase A₂. *Arch. Biochem. Biophys.* **284**, 352–359
- Scott, D. L., Achari, A., Vidal, J. C. and Sigler, P. B. (1992) Crystallographic and biochemical studies of the (inactive) Lys-49 phospholipase A₂ from the venom of *Agkistrodon piscivorus piscivorus*. *J. Biol. Chem.* **267**, 22645–22657
- Cintra, A. C., Marangoni, S., Oliveira, B. and Giglio, J. R. (1993) Bothropstoxin-I: amino acid sequence and function. *J. Protein Chem.* **12**, 57–64
- van den Bergh, C. J., Slotboom, A. J., Verheij, H. M. and de Haas, G. H. (1988) The role of aspartic acid-49 in the active site of phospholipase A₂. A site-specific mutagenesis study of porcine pancreatic phospholipase A₂ and the rationale of the enzymatic activity of lysine-49 phospholipase A₂ from *Agkistrodon piscivorus piscivorus* venom. *Eur. J. Biochem.* **176**, 353–357
- Li, Y., Yu, B. Z., Zhu, H., Jain, M. K. and Tsai, M. D. (1994) Phospholipase A₂ engineering. Structural and functional roles of the highly conserved active site residue aspartate-49. *Biochemistry* **33**, 14714–14722
- Yu, B. Z., Rogers, J., Tsai, M. D., Pidgeon, C. and Jain, M. K. (1999) Contributions of residues of pancreatic phospholipase A₂ to interfacial binding, catalysis, and activation. *Biochemistry* **38**, 4875–4884
- Shimohigashi, Y., Tani, A., Matsumoto, H., Nakashima, K. and Yamaguchi, Y. (1995) Lysine-49 phospholipases A₂ from *Trimeresurus flavoviridis* venom are membrane-acting enzymes. *J. Biochem. (Tokyo)* **118**, 1037–1044
- Yamaguchi, Y., Shimohigashi, Y., Chiwata, T., Tani, A., Chijiwa, T., Lomonte, B. and Ohno, M. (1997) Lys-49 phospholipases A₂ as active enzyme for β-arachidonoyl phospholipid bilayer membranes. *Biochem. Mol. Biol. Int.* **43**, 19–26
- Mancin, A. C., Soares, A. M., Giglio, C. A., Andrião-Escarso, S. H., Vieira, C. A. and Giglio, J. R. (1997) The histamine releasers crotamine, protamine and compound 48/80 activate specific proteases and phospholipases A₂. *Biochem. Mol. Biol. Int.* **42**, 1171–1177
- Holland, D. R., Clancy, L. L., Muchmore, S. W., Ryde, T. J., Einspahr, H. M., Finzel, B. C., Heinrickson, R. L. and Watenpaugh, K. D. (1990) The crystal structure of a lysine 49 phospholipase A₂ from the venom of the cottonmouth snake at 2.0 Å resolution. *J. Biol. Chem.* **265**, 17649–17656
- Arni, R. K., Ward, R. J., Gutiérrez, J. M. and Tulinsky, A. (1995) Structure of a calcium-independent phospholipase-like myotoxic protein from *Bothrops asper* venom. *Acta Crystallogr. Ser. D: Biol. Crystallogr.* **51**, 311–317
- da Silva Giotto, M. T., Garratt, R. C., Oliva, G., Mascarenhas, Y. P., Giglio, J. R., Cintra, A. C. O., Arni, R. K. and Ward, R. J. (1998) Crystallographic and spectroscopic characterization of a molecular hinge: conformation changes in Bothropstoxin-I, a dimeric Lys-49 phospholipase A₂ homologue. *Protein Struct. Funct. Genet.* **30**, 442–455
- de Azevedo, Jr, W. F., Ward, R. J., Canduri, F., Soares, A., Giglio, J. R. and Arni, R. K. (1998) Crystal structure of piratoxin-I: a calcium-independent, myotoxic phospholipase A₂-homologue from *Bothrops pirajai* venom. *Toxicon* **36**, 1395–1406
- de Azevedo, W. F., Ward, R. J., Gutierrez, J. M. and Arni, R. K. (1999) Structure of a Lys49-phospholipase A₂ homologue isolated from the venom of *Bothrops nummifer* (jumping viper). *Toxicon* **37**, 371–384
- Arni, R. K., Fontes, M. R., Barberato, C., Gutierrez, J. M., Diaz, C. and Ward, R. J. (1999) Crystal structure of myotoxin II, a monomeric Lys49-phospholipase A₂ homologue isolated from the venom of *Cerrophidion (Bothrops) godmani*. *Arch. Biochem. Biophys.* **366**, 177–182
- Lee, W. H., da Silva Giotto, M. T., Marangoni, S., Toyama, M. H., Polikarpov, I. and Garratt, R. C. (2001) Structural basis for low catalytic activity in Lys49 phospholipases A₂ – a hypothesis: the crystal structure of piratoxin II complexed to fatty acid. *Biochemistry* **40**, 28–36
- Scott, D. L. and Sigler, P. B. (1994) Structure and catalytic mechanism of secretory phospholipases A₂. *Adv. Protein Chem.* **45**, 53–88
- Díaz, C., Gutiérrez, J. M., Lomonte, B. and Gene, J. A. (1991) The effect of myotoxins isolated from *Bothrops* snake venoms on multilamellar liposomes: relationship to phospholipase A₂, anticoagulant and myotoxic activities. *Biochim. Biophys. Acta* **1070**, 455–460
- Rufini, S., Cesaroni, P., Desideri, A., Farias, R., Gubensek, F., Gutiérrez, J. M., Luly, P., Massoud, R., Morero, R. and Pedersen, J. Z. (1992) Calcium ion independent membrane leakage induced by phospholipase-like myotoxins. *Biochemistry* **31**, 12424–12430
- Pedersen, J. Z., de Arcuri, B. F., Moreno, R. D. and Rufini, S. (1994) Phospholipase-like myotoxins induce rapid membrane leakage of non-hydrolyzable ether-lipid liposomes. *Biochim. Biophys. Acta* **1190**, 177–180
- Homsí-Brandenburg, M. I., Queiroz, L. S., Santo-Neto, H., Rodrigues-Simoni, L. and Giglio, J. R. (1988) Fractionation of *Bothrops jararacussu* snake venom: partial chemical characterization and biological activity of bothropstoxin. *Toxicon* **26**, 615–627

- 33 Ward, R. J., de Oliveira, A. H. C., Bortoleto, R. K., Rosa, J. C., Faça, V. M. and Greene, L. J. (2001) Expression and the purification of a disulphide rich protein in a hydrophobic resin environment: Bothropstoxin-I, a Lys49-phospholipase A₂ homologue. *Protein Expr. Purif.* **21**, 134–140
- 34 Ward, R. J., Monesi, N., Arni, R. K., Larson, R. E. and Paço-Larson, M. L. (1995) Sequence of a cDNA encoding bothropstoxin I, a myotoxin from the venom of *Bothrops jararacussu*. *Gene* **156**, 305–306
- 35 Deng, W. P. and Nickoloff, J. A. (1992) Site-directed mutagenesis of virtually any plasmid by eliminating a unique site. *Anal. Biochem.* **200**, 81–88
- 36 Heinrichson, R. L. (1991) Dissection and sequence analysis of phospholipase A₂. *Methods Enzymol.* **197**, 201–215
- 37 Nelson, R. M. and Long, G. L. (1989) A general method of site-specific mutagenesis using a modification of the *Thermus aquaticus* polymerase chain reaction. *Anal. Biochem.* **180**, 147–151
- 38 de Oliveira, A. H. C., Giglio, J. R., Andriao-Escarso, S. H., Ito, A. S. and Ward, R. J. (2001) A pH-induced dissociation of the dimeric form of a lysine 49-phospholipase A₂ abolishes Ca²⁺-independent membrane-damaging activity. *Biochemistry* **40**, 6912–6920
- 39 Lobo de Araujo, A. and Radvanyi, F. (1987) Determination of phospholipase A₂ activity by a colorimetric assay using a pH indicator. *Toxicon* **25**, 1181–1188
- 40 de Oliveira, A. H. C., Giglio, J. R., Andriao-Escarso, S. H., Ito, A. S. and Ward, R. J. (2001) The effect of resonance energy homotransfer on the intrinsic tryptophan fluorescence emission of the bothropstoxin-I dimer. *Biochem. Biophys. Res. Commun.* **284**, 1011–1015
- 41 Sekar, K., Biswas, R., Li, Y., Tsai, M. and Sundaralingam, M. (1999) Structures of the catalytic site mutants D99A and H48Q and the calcium-loop mutant D49E of phospholipase A₂. *Acta Crystallogr. Sect. D: Biol. Crystallogr.* **55**, 443–447
- 42 Andriao-Escarso, S. H., Soares, A. M., Rodrigues, V. M., Angulo, Y., Diaz, C., Lomonte, B., Gutierrez, J. M. and Giglio, J. R. (2000) Myotoxic phospholipases A₂ in bothrops snake venoms: effect of chemical modifications on the enzymatic and pharmacological properties of bothropstoxins from *Bothrops jararacussu*. *Biochimie* **82**, 755–763
- 43 Kinkaid, A. R. and Wilton, D. C. (1995) Enhanced hydrolysis of phosphatidylcholine by group II non-pancreatic secreted phospholipase A₂ as a result of an interfacial activation by specific anions. *Biochem. J.* **308**, 507–512
- 44 Ownby, C. L., Selistre de Araujo, S. H., White, S. P. and Fletcher, J. E. (1999) Lysine 49 phospholipase A₂ proteins. *Toxicon* **37**, 411–445
- 45 Fletcher, J. E. and Jiang, M. S. (1998) Lys49 phospholipase A₂ myotoxins lyse cell cultures by two distinct mechanisms. *Toxicon* **36**, 1549–1555
- 46 van den Bergh, C. J., Slotboom, A. J., Verheij, H. M. and de Haas, G. H. (1989) The role of Asp-49 and other conserved amino acids in phospholipases A₂ and their importance for enzymatic activity. *J. Cell. Biochem.* **39**, 379–390
- 47 Janssen, M. J., van de Wiel, W. A., Beiboer, S. H., van Kampen, M. D., Verheij, H. M., Slotboom, A. J. and Egmond, M. R. (1999) Catalytic role of the active site histidine of porcine pancreatic phospholipase A₂ probed by the variants H48Q, H48N and H48K. *Protein Eng.* **12**, 497–503
- 48 Pedersen, J. Z., Lomonte, B., Massoud, R., Gubensek, F., Gutierrez, J. M. and Rufini, S. (1995) Autocatalytic acylation of phospholipase-like myotoxins. *Biochemistry* **34**, 4670–4675
- 49 Soares, A. M., Guerra-Sá, R., Borja-Oliveira, C. R., Rodrigues, V. M., Rodrigues-Simioni, L., Rodrigues, V., Fontes, M. R., Lomonte, B., Gutierrez, J. M. and Giglio, J. R. (2000) Structural and functional characterization of BnSP-7, a Lys49 myotoxic phospholipase A₂ homologue from *Bothrops neuwiedi* pauloensis venom. *Arch. Biochem. Biophys.* **378**, 201–209
- 50 Toyama, M. H., Soares, A. M., Vieira, C. A., Novello, J. C., Oliveira, B., Giglio, J. R. and Marangoni, S. (1998) Amino acid sequence of piratoxin-I, a myotoxin from *Bothrops pirajai* snake venom, and its biological activity after alkylation with p-bromophenacyl bromide. *J. Protein Chem.* **17**, 713–718
- 51 Soares, A. M., Andriao-Escarso, S. H., Bortoleto, R. K., Rodrigues-Simioni, L., Arni, R. K., Ward, R. J., Gutierrez, J. M. and Giglio, J. R. (2001) Dissociation of enzymatic and pharmacological properties of piratoxins-I and -III, two myotoxic phospholipases A₂ from *Bothrops pirajai* snake venom. *Arch. Biochem. Biophys.* **387**, 188–196
- 52 Fletcher, J. E., Hubert, M., Wieland, S. L., Gong, Q.-H. and Jiang, M.-S. (1996) Similarities and differences in mechanisms of cardiotoxins, melittin and other myotoxins. *Toxicon* **34**, 1301–1311
- 53 Calderon, L. and Lomonte, B. (1998) Immunochemical characterization and role in toxic activities of region 115–129 of myotoxin II, a Lys49 phospholipase A₂ from *Bothrops asper* snake venom. *Arch. Biochem. Biophys.* **358**, 343–350
- 54 Lomonte, B., Pizarro-Cerda, J., Angulo, Y., Gorvel, J. P. and Moreno, E. (1999) Tyr → Trp-substituted peptide 115–129 of a Lys49 phospholipase A₂ expresses enhanced membrane-damaging activities and reproduces its *in vivo* myotoxic effect. *Biochim. Biophys. Acta* **1461**, 19–26
- 55 Ward, R. J., Alves, A. R., Ruggiero Neto, J., Arni, R. K. and Casari, G. A. (1998) SequenceSpace analysis of Lys49 phospholipases A₂: clues towards identification of residues involved in a novel mechanism of membrane damage and in myotoxicity. *Protein Eng.* **11**, 285–294
- 56 Selistre de Araujo, H. S., Withe, S. P. and Ownby, C. L. (1996) Sequence analysis of Lys49 phospholipase A₂ myotoxins. *Toxicon* **34**, 1237–1242
- 57 Guex, N. and Peitsch, M. C. (1997) SWISS-MODEL and the Swiss-PDB Viewer: an environment for comparative protein modeling. *Electrophoresis* **18**, 2714–2723

Received 18 September 2001/31 October 2001; accepted 29 November 2001